

Theoretical study of structure and reactions of metalated oximes and oxime ethers

Rainer Glaser and Andrew Streitwieser, Jr.

Department of Chemistry, University of California, Berkeley, CA 94720

Abstract - The potential energy surfaces of acetaldoxime carbanion and its ion pairs formed with lithium and sodium cations ions have been explored with *ab initio* methods to model and study the regiochemistry of metalated oxime ethers. Planar structures of the carbanions produced by deprotonating acetaldoxime are minima on the potential energy surface. The *syn*-isomer is 2.6 Kcal/mole more stable than the *anti*. This difference is not a manifestation of cyclic conjugation but more likely is a result of electrostatic effects. Two chiral and almost isoenergetic minima have been located for the ion pairs formed by either of the isomeric carbanions with Li^+ or Na^+ . The nitrogen engages either in face coordination or bridges the NO-bond in a η^2 -fashion. In oxime ethers face coordination is expected to become dominant for steric reasons. LIC-contacts are surprisingly long in all of the ion pairs. Bonding to the metals in the ion pairs is predominantly ionic. Ion pair formation increases the *syn* preference energy compared to the free anions, and the *syn* preference energy is greater for Na^+ than for Li^+ . Reactions with electrophiles via the *syn*-coordinated metal permits prior coordination and ion pair formation in the product.

INTRODUCTION

The formation of a new carbon-carbon bond in the α -position to a carbonyl group is one of the most important reactions of modern synthetic organic chemistry but the control of the regiochemistry is an especial problem that has received much recent attention. The introduction of metalated enolate equivalents (ref. 1-3) has resolved many of these problems and opened a wide field of modern synthetic chemistry (ref. 4). Many metalated N-derivatives of carbonyl compounds, $\text{R}_1\text{R}_2\text{C}=\text{N}-\text{X}$, have been used as enolate equivalents. Oxime ethers are typical examples (ref. 5-8) and form the basis for the present study.

One of the most important characteristics of these organometallic reagents is the high regioselectivity of their formation; a remarkable preference for the *syn*-configured enolate is generally observed (ref. 9,10). In a typical reaction sequence the N-derivative of the carbonyl compound is generated, deprotonated with a strong metallorganic base (BuLi , LDA, LDEA, KDA and others) at low temperature in THF and reacted with the electrophilic reagent. This sequence, terminated by the regeneration of the carbonyl function, has been successfully used to produce a great variety of synthetically valuable mono-, bis- and polyfunctional molecules under mild conditions and in high yields. Carbon-carbon bond formations by oxidative addition of the enolate intermediate have also been reported (ref. 3,8). Since the reactions involve relatively non-polar solvents, such as ethers, ion pairs rather than free carbanions are clearly implicated. Low temperature deprotonations also raise the question of whether the *syn*-regiochemistry found is a kinetic rather than a thermodynamic phenomenon.

These questions are studied in the present work with *ab initio* calculations of isomeric carbanions of oximes and their monomeric lithium and sodium derivatives as models for metalated oxime ethers (ref. 11). Some reaction transition structures have also been determined for these compounds. The role of aggregated intermediates in these reactions has not been settled (ref. 12, 13); most recent discussions have assigned a primary role to the monomeric metalated species.

METHODS

Standard single-determinant spin-restricted Hartree-Fock calculations were performed with the programs GAUSSIAN 80 and GAUSSIAN 82 (ref. 14). Structures of stationary points were optimized simultaneously using analytical gradient techniques (ref. 15). Optimizations were carried out under the constraints of the symmetry point group specified. Because of the sizes of the systems, the considerable numbers of internal degrees of freedom and the shallow nature of the energy surfaces of ion pairs studied the split-valence but still relatively small 3-21G basis set (ref. 16) was used for the structural optimizations. For the calculation of the carbanions the 3-21G basis set was augmented by single diffuse sp-shells (ref. 17-19). The metal cations were described by the 3-21G basis set to provide a more balanced functional description of the paired ions (ref. 20). Energies were calculated with these geometries and the 6-31G* basis set (ref. 21). The standard 6-31G* basis set was modified in that no d-functions were used for the description of the metal atoms. These functions are not necessary for the proper description of the metal cations but would increase the number of empty orbitals at the metal atoms and lead to increased basis set superposition (ref. 20). The 6-31G* basis set was augmented by diffuse sp-shells as in the case of the 3-21G basis set to give the 6-31+G* basis set. Harmonic vibrational frequencies were calculated at the level of optimization to characterize stationary points as minima or saddle points and to obtain vibrational zero-point energies. The vibrational zero-point energy corrections to relative energies were scaled by 0.9 (ref. 22).

Projected electron density functions $P(x,z)$ were calculated with the program PROJ (ref. 23). Demarkation of spatial regions (ref. 24) of $P(x,z)$ and integrations of the contained projected density yield Integrated Projection Populations (IPP). Populations thus obtained are good approximations (ref. 25) to Bader's atomic populations (ref. 26). The electrostatic properties of the carbanions were evaluated with the program MEPHISTO (ref. 27).

The *ab initio* calculations were carried out in part on our VAX-11/750, the VAX-8800 of the Campus Computer Facility and the Cray II at the San Diego Supercomputer Center.

RESULTS AND DISCUSSION

Formaldoxime and Acetaldoxime

The structures of formaldoxime, **1**, and of two methyl rotomers each of Z-, **2**, and E-, **3**, acetaldoxime, were optimized at the 3-21G level. The 6-31G* energies of the structures are summarized in Table 1. These structures will be discussed elsewhere (ref. 25).

Structures, Bonding and Relative Energies of the Isolated Carbanions

Two C_s -symmetric planar structures are minima on the potential energy surface, **4**, in which the deprotonated carbon atom and the hydroxyl group are *syn*, and **5**, in which they are *anti*. The structures are summarized in Fig. 1 and their energies are given in Table 1.

A *syn*-preference energy of 2.6 Kcal/mole has been found for the carbanions of acetaldoxime at 6-31+G*/3-21+G. This SPE is reduced to 2.0 Kcal/mole when vibrational zero-point corrections are taken into account. The *syn*-preference is more pronounced for the carbanions of acetketoxime for which an SPE of 7.3 Kcal/mole has been determined. The proton affinity of **4** (**5**) with respect to **2** (**3**) is 390.1 (392.7) Kcal/mole at 6-31+G*/3-21+G. The difference of 2.4 Kcal/mole between the proton affinities of **4** and **5** represents a quantitative measure of the change in the *syn*-preference energy associated with deprotonation.

Electronic structure of oxime carbanions.

The additional stabilization of the *syn*-carbanion has usually been considered to be caused by homocyclic conjugation. Analysis of the projected electron density function suggests that such conjugation is unimportant. The hydroxyl-O and the C(C)-atom have AO-coefficients in the HOMOs that are of comparable magnitude and with the proper phase to allow for 1,4-through-space overlap in the *syn*-carbanions. These features are necessary but not sufficient requirements to produce sufficient overlap that mediates homocyclic conjugation. The contour map of the projection electron density function of the *syn*-carbanion of acetal-

TABLE 1. Energies as obtained at 3-21+G and 6-31+G*/3-21+G^a and vibrational zero-point energies calculated at the level of optimization.

Molecule ^b and Symmetry	-Energy ^a (au)		
	3-21+G	6-31+G*/3-21+G	ZPE ^c
1, C _s HONCH ₂	167.897520	168.840999	
2a, C _s Z-HONCHCH ₃	206.725238	207.879341	
2b, C _s	206.725048	207.879498	
3a, C _s E-HONCHCH ₃	206.724687	207.880600	
3b, C _s	206.721957	207.877484	
4, C _s <i>syn</i> -X ⁻	206.150687	207.257410	38.91
5, C _s <i>anti</i> -X ⁻	206.148192	207.253275	38.27
6a, C ₁ <i>syn</i> -X ⁻ Li ⁺	213.605497	214.751871	41.42
6b, C ₁ <i>syn</i> -X ⁻ Li ⁺	213.609381	214.751743	41.29
7a, C ₁ <i>anti</i> -X ⁻ Li ⁺	213.590698	214.746764	41.03
7b, C ₁ <i>anti</i> -X ⁻ Li ⁺	213.604659	214.746844	40.97
8a, C ₁ <i>syn</i> -X ⁻ Na ⁺	367.074814	369.132453	41.39
8b, C ₁ <i>syn</i> -X ⁻ Na ⁺	367.074562	369.129062	41.03
9a, C ₁ <i>anti</i> -X ⁻ Na ⁺	367.057732	369.121241	40.40
9b, C ₁ <i>anti</i> -X ⁻ Na ⁺	367.066987	369.121327	40.21

^aMolecules 1-3 were calculated without augmentation by diffuse functions.

^bHONCHCH₂⁻ = X⁻.

^cUnscaled.

doxime (Fig. 2) shows no significant amount of electron density between the hydroxyl-O and the CH₂-carbon. If there were a significant amount of 1,4-overlap then a bond path would exist between the carbanionic center and the oxygen atom and the electron density cross-section in the molecular plane would exhibit a critical point of rank 3 and signature +1, (3,+1), in the center of the cyclic π -system and a critical point of rank 3 and signature -1 along the bond path (ref. 26). The projection of the 3-dimensional electron density into the molecular plane would lead to the corresponding projected critical points (2,+2)_p and (2,0)_p of the projected electron density distribution (ref. 25). These projected critical points are not present in the projected electron density function of the *syn*-carbanion of acetaldoxime. We suggest that the most reasonable explanation for the *syn* preference of the carbanions is the electrostatic repulsion between the nitrogen lone pair and the carbanion carbon which are farther apart in the

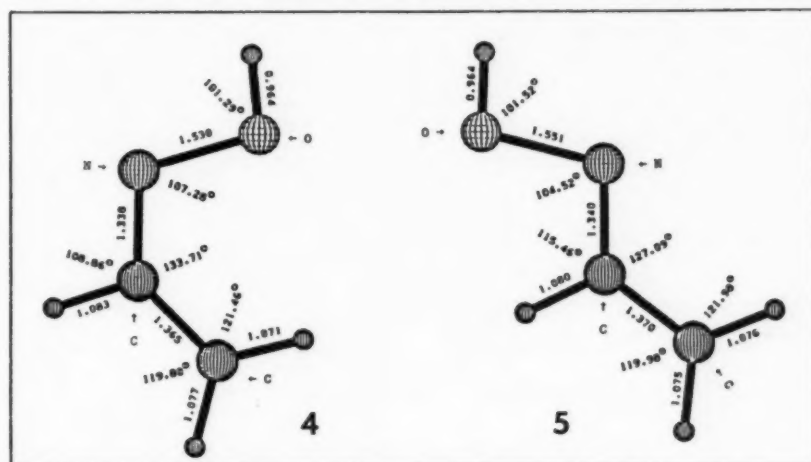


Fig. 1. Optimized structures of isomeric planar carbanions of acetaldoxime, 4 (*syn*, left) and 5 (*anti*, right).

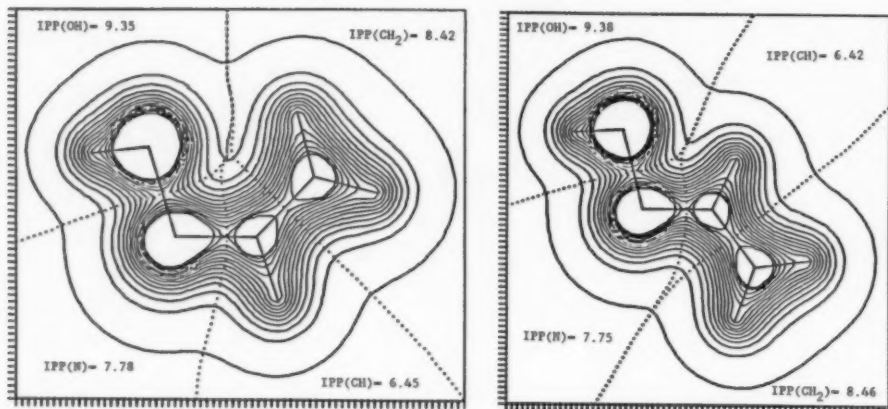


Fig. 2. Contour diagrams of the projected electron density functions of the *syn* (**4**, left) and the *anti* (**5**, right) carbanions of acetaldoxime. Contour levels start at $0.005 \text{ e a.u.}^{-2}$ with a level spacing of 0.05 .

syn-carbanion. However, one has to keep in mind that the energy difference is small and is undoubtedly the result of a delicate balance of a manifold of factors (structure, electronic structure, electrostatic properties of the wavefunction) and all of these factors are different in the isomeric molecules.

One of the most important properties of the oxime carbanions is their charge distribution since the charge distribution is the dominant factor that determines the structures of the ion pairs. The electron density analysis of the isomeric carbanions **4** and **5** reveals that most of the charge is localized on the heteroatoms (Fig. 2) and on nitrogen in particular. The IPP-values of the nitrogen atom and of the hydroxy-group are -0.78 (-0.75) and -0.35 (-0.38) in **4** (**5**), respectively. The charges of the carbanionic carbon atoms are -0.42 (**4**) and -0.46 (**5**) and they are much smaller than the charges on nitrogen. Note that the total negative charge of the HON-fragment is slightly greater than unity. The resulting charge distribution thus indicates localization of most of the anionic charge on the heteroatoms. The negative charge on the terminal CH_2 -group results in part from intramolecular charge transfer from the CH -unit to the CH_2 -group; that is, the charge on the HON-fragment polarizes the CHCH_2 -fragment.

Lithium and sodium ion pairs of oxime carbanions.

All minima of the lithium and sodium ion pairs have been found to be chiral (C_1). For each of the ion pairs formed by the *syn*- or the *anti*-configured carbanions of acetaldoxime two topologically different minima have been located. The metal cation engages either in a formal η^4 - (*syn*) or η^3 - (*anti*) face coordination or bridges the NO-bond in a η^2 -fashion. The structures of the lithium ion pairs of the *syn*- (**6a**, η^4 -face coordination; **6b**, η^2 -NO-bond coordination) and the *anti*-configured carbanions (**7a**, η^3 -face coordination; **7b**, η^2 -NO-bond coordination) of acetaldoxime are shown in Fig. 3. Other stationary structures have been found for the lithium ion pairs of the carbanions of acetaldoxime. All of these stationary structures represent either second-order saddle points or transition state structures for the isomerisation of ion pairs with different hapticity of the metal coordination, for racemization of enantiomeric ion pairs or for the interconversion of *syn/anti*-isomers.

Drawings of the corresponding sodium derivatives are shown in Fig. 4; *syn*-configured isomers **8a** (face coordination) and **8b** (NO-bond coordination), and *anti*-configured isomers **9a** (face coordination) and **9b** (NO-bond coordination).

The lithium cation assumes a bridging position that results in formal η^3 -coordination in the *anti*-configured ion pair **7a**. The LiN-distance is 1.87 \AA and the distance between Li^+ and the carbanionic carbon is considerably longer, 2.27 \AA . In the *syn*-configured molecule **6a** lithium coordinates in a

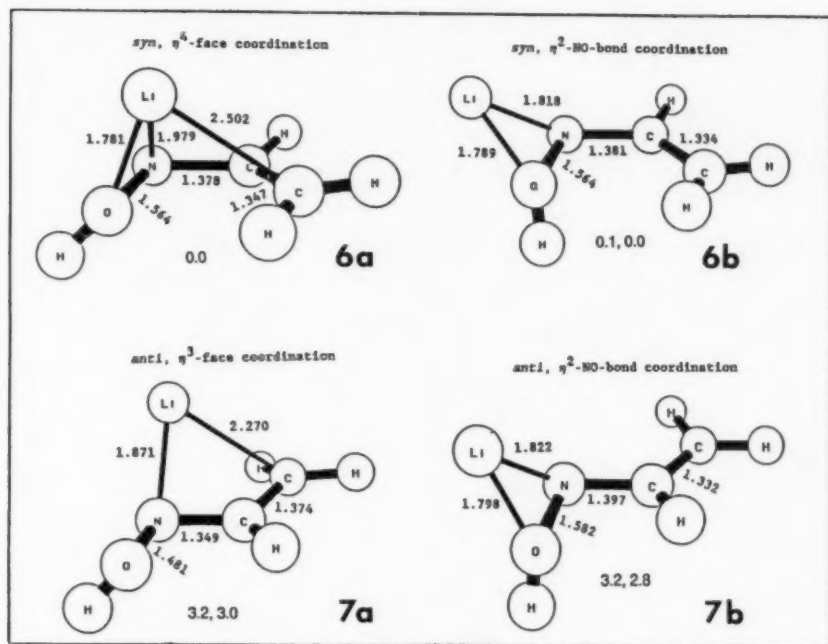


Fig. 3. Molecular models of the chiral lithium ion pairs of isomeric acetaldoxime carbanions. Numbers are relative energies in Kcal/mole based on 6-31+G*/3-21+G SCF calculations; the second number in each pair includes correction for zero point energy.

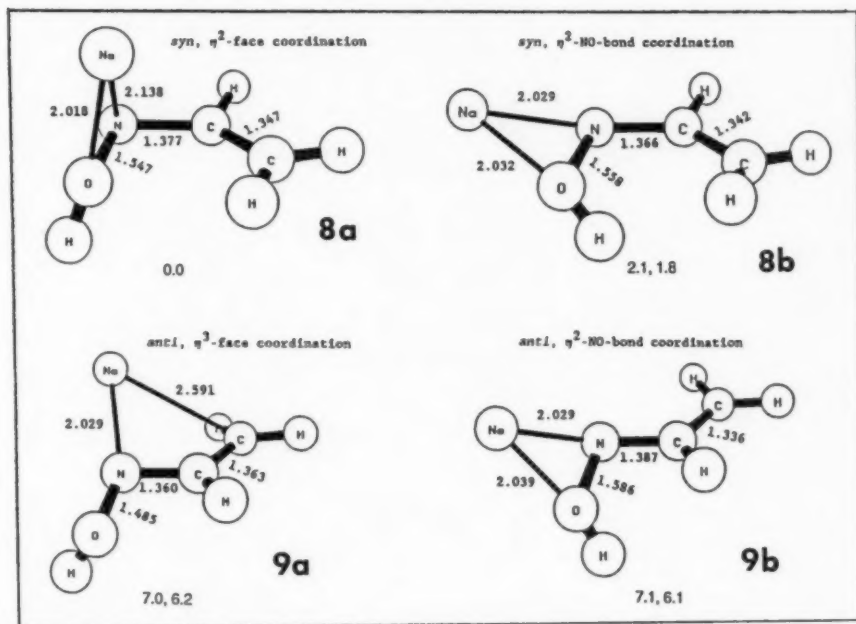


Fig. 4. Sodium ion pairs of isomeric acetaldoxime carbanions. Relative energies are given as in Fig. 3.

η^4 -fashion. This ion pair contains a characteristic triangular arrangement formed by Li^+ in bridging the NO-bond. The LiO- and LiN- distances are 1.78 Å and 1.98 Å, respectively, and the distance between Li^+ and the carbanionic carbon is remarkably long, 2.50 Å. The short distances to the heteroatom(s) indicate the dominant role of the heteroatom(s) in the determination of the position of the cation, whereas the LiC- contact is less important. Although the LiC- distance becomes significantly shortened in the *anti*-configured ion pairs, due to the lack of oxygen chelation, the lithium bridges in a highly unsymmetrical fashion.

The electrostatic potentials of **4** and **5** are especially revealing as to why the cations assume the positions found in the calculations of the ion pairs. Figures 5 and 6 are contour maps of the electrostatic potentials with inclusion of polarization corrections for **4** and **5**, respectively, for planes that are parallel to the molecular plane (*xy*-plane) of the carbanions and at *z*-values approximately those of the lithium. The circles drawn correspond to the closest normal approach of lithium to the ligand atoms (O: 1.8 Å; N: 1.9 Å; C: 2.0 Å). The maximum electrostatic stabilization consistent with these distances is found at points close to the actual positions of lithium optimized for the fixed carbanions (marked **Li** in the figures). These close agreements provide compelling evidence for the dominantly ionic nature of the bonds to lithium in the ion pairs.

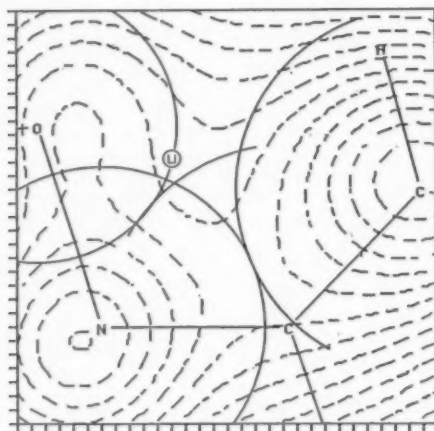


Fig. 5. Electrostatic potential for **4** 1.5 Å from the molecular plane. Contours start at -0.34 au with a level spacing of 0.01 au.

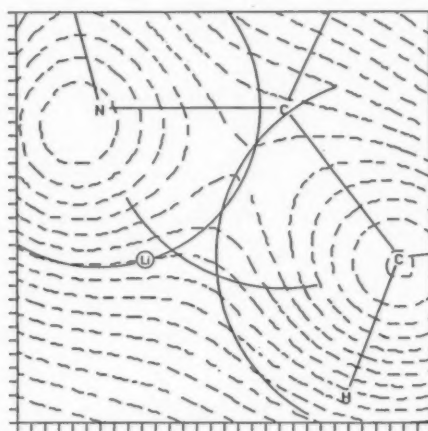


Fig. 6. Electrostatic potential for **5** as in Fig. 5.

The tendency of the gegenion to assume a position as close to the heteroatom(s) as possible is enhanced for Na^+ as compared to Li^+ . In the sodium ion pair of *syn*-configured acetaldoxime, **8a**, the NaO- , NaN- and NaC(C)- distances are 2.02, 2.14 and 3.05 Å, respectively. The increase in bondlengths between the heteroatoms and sodium as compared to lithium ($\Delta(\text{M-O}) = 0.24$ Å, $\Delta(\text{M-N}) = 0.16$ Å) is less than the difference in the ionic radii of the alkali metals, 0.29 Å, whereas the opposite is true for the carbon-metal bond ($\Delta(\text{M-C}) = 0.45$ Å). The NaN- and NaC(C)- distances in the *anti*-configured sodium ion pair, **9a**, are 2.03 and 2.59 Å, respectively. The large reduction of the NaC- distance by 0.46 Å compared to the *syn*-configured isomer **8a** demonstrates the increased importance of the metal-carbon contact when the hydroxyl-O is not available for chelation. The MN- distance is only lengthened by 0.16 Å compared to **7a**, whereas the MC- distance is lengthened by twice that amount. Replacement of Li^+ by Na^+ does not give simple changes in bond distances. Sodium assumes an equilibrium position in **8a** in which the ONNa- and the NCC- planes are almost perpendicular, whereas the plane defined by the NO-bond and lithium is significantly bent toward the CH_2 -group in the corresponding lithium ion pairs. The resulting coordination in the sodium case is thus more a η^2 -coordination of the heteroatoms rather than a η^4 -face coordination.

The η^2 -NO-bond coordinated structures are best described as metalated vinyl-substituted hydroxylimides. NO-bond coordination results in greatly shortened metal-nitrogen bond distances compared to face coordination. The Li-N bond length in the *syn*-configured ion pair **6b** is 0.16 Å shorter than in **6a** and the Na-N bond length in **8b** is 0.11 Å shorter than in **8a**. The M-O bond distances are virtually identical for the lithium ion pairs of the *syn*-configured carbanion and the Na-O bond distance in **8b** is only slightly increased compared to **8a**. A shortening of the MN-bond in the lithium ion pair of the *anti*-configured carbanion (1.87 Å in **6a**, 1.82 Å in **6b**) is less significant and the Na-N bond is 2.03 Å in both sodium derivatives **9a** and **9b**. The differences of the bond lengths between the heteroatoms and sodium compared to lithium show the same trend as for the face coordinated ion pairs. Replacement of Li^+ by Na^+ causes increases of the MN- and MO-bond lengths ($\Delta(\text{M-N}) = 0.21$ Å, $\Delta(\text{M-O}) = 0.24$ Å) that are smaller than the difference of ionic radii of the alkali metals (0.29 Å). The CN-bond lengthens by 0.05 Å and the CC-bond shortens by 0.04 Å in going from face to NO-bond coordination in the *anti*-configured lithium ion pair. These structural alternations are in agreement with the reorganization of the the aza-allyl type electronic structure in **7a** to the vinylimide type structure in **7b** and they also show that the charge delocalization within the anion depends to some extent on the position of the gegenion. Surprisingly, the change of coordination mode in the *syn*-configured ion pairs **6a** and **6b** leaves the CN-bond length unchanged and the CC-bond length is affected but little (0.02 Å). This finding indicates that the formally η^4 -face coordinated species **6a** might be better described as a second version of the η^2 -NO-bond coordinated ion pair. Similar trends are observed for the bond length alterations in the isomeric sodium ion pairs.

Relative energies and *syn*-preference energies.

The lithium and sodium ion pairs formed with the same geometrical isomer of the acetaldoxime carbanion but with different hapticities are essentially isoenergetic. Only the sodium ion pairs of the *syn*-configured carbanion show a preference for one of the isomeric ion pairs; the formally face coordinated ion pair **8a** is favored over ion pair **8b** by 1.8 Kcal/mole. Replacement of the hydroxy-group by an alkoxy group is not expected to affect the face coordinated ion pairs to a great extent. In all of the optimized ion pair structures with the gegenion engaged in a face coordination the orientation of the hydroxyl group is such that the introduction of the alkyl group should be sterically unhindered. The relative energies of the face coordinated ion pairs are therefore expected to carry over from metalated oximes to metalated oxime ethers. In contrast, the η^2 -NO-bond coordinated ion pairs may be affected by such a replacement. Introduction of an alkyl group into the sodium ion pairs **9b** and **9c** would probably destabilize these ion pairs due to steric repulsion. In the case of the *syn*-configured ion pair, the alkoxy group may perhaps even cause the NO-bridged structure to vanish as a local minimum of the potential energy surface. The NO-bridged lithium ion pairs are comparatively less subject to steric destabilization since the β -angles are larger. In any case, it is reasonable to assume that the ion pairs involving face coordination are energetically favored over η^2 -NO-bond coordinated ion pairs for metalated oxime ethers. The following discussion of the *syn* preference energies therefore refers to the face coordinated ion pairs.

The $6-31+G^*/3-21+G$ *syn*-preference energy (SPE) is 2.6 Kcal/mole for the isolated carbanions of acetaldoxime. Ion pair formation increases the SPE to 3.2 Kcal/mole for Li^+ and 7.0 Kcal/mole for Na^+ . Consideration of vibrational zero-point energy corrections gives slightly smaller SPE-values; 2.0 Kcal/mole for the anions, 3.0 Kcal/mole for the lithium ion pairs, and 6.2 Kcal/mole for the sodium derivatives. These results suggest that bases with larger cations may achieve increased regioselectivity.

Reactions with electrophiles.

A number of transition structures have been found for the lithium ion pairs and will be discussed elsewhere (ref. 25). The lithium ion pairs are chiral and can interconvert or racemize by several mechanisms. One of the racemization mechanisms has been found to involve chiral transition states. All of these processes occur with only small barriers and should be facile. Thus, any of these structures is readily available as a reaction intermediate. In reactions with electrophilic reagents, coordination with lithium has frequently been invoked as an essential part of the sequence (ref. 28). Such prior coordination would generally imply reaction with the electrophile at the same side as the lithium although alternative stereochemistries have been proposed (ref. 12). Moreover, cases are known in which protonation and alkylation occur at different sides

of a lithium coordinated carbanion (ref. 29). We have studied theoretically the reaction of the lithium ion pair of the *syn*-carbanion of acetaldoxime with hydrogen fluoride leading to acetaldoxime and lithium fluoride. The hydrogen fluoride was allowed to approach the molecule from the same side as lithium (*cis*) and from the opposite side (*trans*). All of the molecules involved in the protonation reaction were calculated with the 3-21G basis set. At this basis set level the reaction is exothermic by 28.2 Kcal/mole. The bond distances between lithium and the skeleton atoms of the anion in the ion pair are significantly reduced at the 3-21G level compared to the 3-21+G calculations. The shortening of these bonds indicates a larger basis set superposition error at 3-21G. The reaction was also studied at 3-21G with the inclusion of a shell of diffuse *sp*-functions on F, 3-21+[F]G. The structural effects are small but energies are affected significantly.

The approach of HF from the metal-coordinated face of the ion pair results in the coordination of HF to the lithium cation followed by orientation of the HF toward the reactive center and reaction without an activation barrier. Optimization of the positions only of Li⁺ and HF while keeping all other parameters those of the isolated lithium ion pair gives a structure that is not a true energy minimum complex but does show a favorable positioning of the HF for reaction with the carbanion. Proton transfer results in the complex between acetaldoxime and lithium fluoride shown in Fig. 7.

Reaction of HF with the ion pair from the side opposite to the metal coordination (*trans*) does not occur in this gas phase model. This result was obtained even with diffuse functions on fluorine. Hydrogen fluoride approaches the reactive center (Fig. 8) but the proton transfer is impeded because it would leave the ions Li⁺ and F⁻ on opposite sides of the reaction product acetaldoxime.

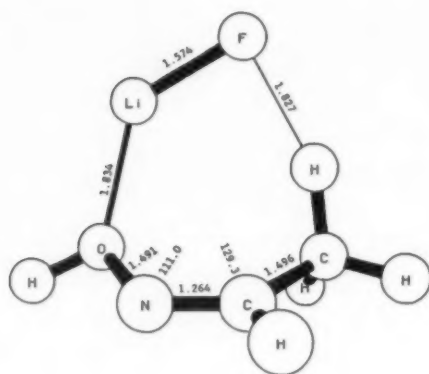


Fig. 7. Product of *cis*-reaction of 6a and HF.

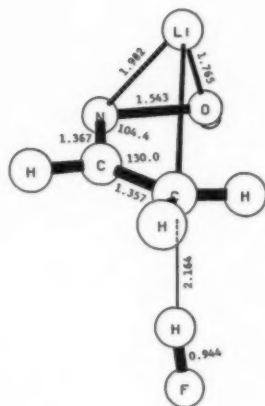


Fig. 8. *Trans*-attack of HF on 6a does not lead to proton transfer.

In solution the exothermicity of the reaction from the *syn*-side would be reduced since the electrophile would have to compete with solvent molecules in order to achieve the precoordination necessary to place fluorine close to the lithium cation. Indeed, the replacement of a coordinating solvent by the more poorly coordinating HF may well contribute to an activation barrier. In contrast, the reaction involving the entry of the electrophile from the opposite side would probably involve different solvation factors. The calculated energies are therefore of little significance. The important point to be made is that lithium cannot pass through the plane of the anion as the electrophile approaches from the opposite side. The inability of the lithium cation to change sides upon *trans*-entry of an electrophile leaves the lithium and the fluoride ions far apart and it seems unlikely that such a situation could be competitive with the ideal arrangement of the reactants in the case of the *cis*-entry.

The above reaction deals only with monomers. A recent MNDO study has indicated that lithiated oxime ether dimers may be present in solution but that reaction with electrophiles probably involves only the monomeric ion pairs. The calculations suggest a general mechanism for the reaction of metalated oxime ethers with electrophiles. Entry of the electrophilic reagent into the primary solvation shell of the gegenion leads to precoordination between the reagent and the metalated oxime ether. Orientation of the reagent initiates reaction and leads to the α -substituted oxime ether. Dissociation of the post-reaction complex between the oxime ether and the lithium salt terminates the reaction sequence.

Acknowledgements

This work was supported in part by NSF grant CHE85-02137, NIH grant GM-30369, and by generous grants of computer time by the San Diego Supercomputer Center and the Campus Computer Facilities, UCB. RG is a fellow of the Fonds der Chemischen Industrie, 1985-7.

REFERENCES

1. G. Wittig, H.D. Frommeld, and P. Suchanek, *Angew. Chem.* **75**, 978 (1963); G. Wittig and H. Reiff, *Angew. Chem.* **80**, 8 (1968); G. Wittig and A. Hesse, *Org. Synth.* **50**, 66 (1970).
2. G. Stork and S.R. Dowd, *J. Am. Chem. Soc.* **85**, 2178 (1963); *Org. Synth.* **50**, 66 (1974).
3. F.E. Henoch, K.G. Hampton and C.R. Hauser, *J. Am. Chem. Soc.* **91**, 676 (1969).
4. For some reviews see: P.W. Hickmott, *Tetrahedron* **14**, 1975 (1982); D. Enders, in J.D. Morrison, *Asymmetric Synthesis*, Vol. 3, p. 275, Academic Press, New York (1984); D. Seebach and H.-K. Geiss, in D. Seyferth, *Journal of Organometallic Chemistry Library 1*; Elsevier, Amsterdam (1976).
5. T.A. Spencer and C.W. Leong, *Tet. Lett.* **45**, 3889 (1975).
6. R.R. Fraser and K.K. Dhawan, *J. Chem. Soc., Chem. Comm.* 674 (1976).
7. R.E. Gawley, E.J. Termine, and J. Aube, *J. Tet. Lett.* **21**, 3115 (1980).
8. S. Shatzmiller and R. Lidor, *Synthesis*, 590 (1983).
9. R. Lidor and S. Shatzmiller, *J. Am. Chem. Soc.* **103**, 5916 (1981).
10. D.E. Bergbreiter and M. Newcomb, *M. Tet. Lett.* **43**, 4145 (1979); J.W. Ludwig, M. Newcomb and D.E. Bergbreiter, *J. Org. Chem.* **45**, 4666 (1980).
11. R. Glaser and A. Streitwieser, Jr., *J. Am. Chem. Soc.* **109**, 1258 (1987).
12. D.B. Collum, D. Kahne, S.A. Gut, R.T. DePue, F. Mohamadi, R.A. Wanat, J. Clardy and G. Van Duyne, *J. Am. Chem. Soc.* **106**, 4865 (1984); R.A. Wanat and D.B. Collum, *J. Am. Chem. Soc.* **107**, 2078 (1985).
13. R. Glaser and A. Streitwieser, Jr., *Theochem.*, submitted.
14. a) GAUSSIAN 80 UCSF: U.C. Singh and P. Kollman, *QCPE Bull.* **2**, 17 (1982); b) J.S. Binkley, M. Frisch, K. Raghavachari, D. DeFrees, B. Schlegel, R. Whiteside, E. Fluder, R. Seeger, and J.A. Pople, GAUSSIAN 82, Release A Version, Carnegie-Mellon University, 1983.
15. H.P. Schlegel, *J. Comput. Chem.* **3**, 214 (1982).
16. J.S. Binkley, J.A. Pople and W.J. Hehre, *J. Am. Chem. Soc.* **102**, 939 (1980); M.S. Gordon, J.S. Binkley, J.A. Pople, W.J. Pietro and W.J. Hehre, *J. Am. Chem. Soc.* **104**, 2197 (1982).
17. L. Radom, *Mod. Theor. Chem.* **4**, 333 (1977); A.D. Hopkinson, *Prog. Theor. Org. Chem.* **2**, 194 (1977).

18. J. Chandrasekhar, J.G. Andrade and P.v.R. Schleyer, J. Am. Chem. Soc. **103**, 5609 (1981), and references therein; G.W. Spitznagel, T. Clark, J. Chandrasekhar and P.v.R. Schleyer, J. Comp. Chem. **3**, 363 (1982); A.-M. Sapse, E. Kaufmann, P.v.R. Schleyer, and R. Gleiter, Inorg. Chem. **23**, 1569 (1984); G. Winkelhofer, R. Janoscsek, F. Fratev, G.W. Spitznagel, J. Chandrasekhar and P.v.R. Schleyer, J. Am. Chem. Soc. **107**, 332 (1985); D. Cremer and E. Kraka, J. Phys. Chem. **90**, 33 (1986), and references therein.
19. T. Clark, J. Chandrasekhar, G.W. Spitznagel and P.v.R. Schleyer, J. Comp. Chem. **3**, 294 (1983).
20. A. Pullman, H. Berthod and N. Gresh, Intern. J. Quantum Chem. **10**, 59 (1976).
21. W.J. Hehre, R. Ditchfield and J.A. Pople, J. Chem. Phys. **56**, 2257 (1972); P.C. Hariharan and J.A. Pople, Theoret. Chim. Acta **28**, 213 (1973).
22. M.M. Francl, W.J. Pietro, W.J. Hehre, M.S. Gordon, D.J. Defrees and J.A. Pople, J. Phys. Chem. **77**, 3654 (1982).
23. A. Streitwieser, Jr., J.B. Collins, J.M. McKelvey, D.L. Grier, J. Sender and A.G. Toczko, Proc. Natl. Acad. Sci. U.S.A. **76**, 2499 (1979); J.B. Collins, A. Streitwieser, Jr., and J. McKelvey, Comput. Chem. **3**, 79 (1979); J.B. Collins and A. Streitwieser, Jr., J. Comput. Chem. **1**, 81 (1980).
24. R.S. McDowell, D.L. Grier and A. Streitwieser, Jr., Comp. & Chem. **9**, 165 (1985).
25. R. Glaser and A. Streitwieser, Jr., manuscript in preparation.
26. R.F.W. Bader, Acc. Chem. Res. **18**, 9 (1985), and references therein.
27. M. Miller Francl, QCPE No. **490**.
28. For a recent review see P. Beak and A.I. Meyers, Accts. Chem. Res., **19**, 356 (1986).
29. A.I. Meyers and D.A. Dickman, J. Am. Chem. Soc., **109**, 1263 (1987); K. Nakamura, M. Higaki, S. Adachi, S. Oka and A. Ohno, J. Org. Chem., **52**, 1414 (1987).